



CHARACTERIZATION OF DIRECTIVITY EFFECTS OBSERVED DURING 1999 CHI-CHI, TAIWAN EARTHQUAKE

Vietanh PHUNG¹, Gail M. ATKINSON² and David T. LAU³

SUMMARY

It has been observed in some recent strong earthquakes that ground motion amplitudes are often enhanced in the direction of fault rupture propagation. Damage pattern observations in the 1999 $M_w=7.6$ Chi-Chi Taiwan earthquake indicated that severe damage was concentrated near and along the fault rupture, particularly in the northern part of the fault. Directivity effects for this thrust earthquake would be expected to enhance ground motions up-dip of the hypocenter. There may also be some directivity to the north, as slip distributions have shown that displacements significantly increased from the south to the north along the fault as the rupture propagated in that direction. This paper aims to quantify the directivity effects on the peak ground acceleration (PGA) and 5%-damped response spectral accelerations (PSA) of strong-motions recorded during the Chi-Chi earthquake. The median relationships of ground motion amplitudes as a function of the closest distance to the fault and site category are determined in the first step, using 420 ground motion time histories recorded on rock and soil sites. Then the residuals (model errors) of these relationships as a function of selected geometrical parameters related to the fault are used to describe the directivity effects. The geometrical parameters include the fraction of the fault rupture that lies between the hypocenter and the site, and the angle between the fault plane and the path from the hypocenter to the site. Since the Chi-Chi earthquake is of thrust type, dip-slip directivity effects as well as along-strike propagation effects are studied. All sites are used to quantify along-strike directivity effects, while only sites within 50 km of the fault rupture are used to quantify dip-slip directivity effects. The dip-slip component of the directivity effects has a strong influence, increasing ground motion amplitudes up dip of the hypocenter by a factor of approximately 2.7. The along-strike effects are also significant: ground motion amplitudes are approximately 1.5 times higher for stations in which rupture propagated strongly towards the site than those for which rupture propagated away from the station. Directivity effects are observed for PGA and PSA at all periods.

INTRODUCTION

At 1:47 AM on Tuesday 21 September 1999 an earthquake of magnitude $M_w=7.6$ hit central Taiwan. The epicenter was located at 23.78° N and 121.09° E near the town of Chi-Chi. After the earthquake, the

¹ Graduate Student, Department of Civil & Environmental Engineering, Carleton University, Canada

² Professor, Department of Earth Science, Carleton University, Canada

³ Professor, Department of Civil & Environmental Engineering, Carleton University, Canada

Central Weather Bureau (Lee *et al.* [1]) successfully retrieved about 420 free-field recordings out of more than 650 strong-motion stations deployed at free-field sites. This wealth of data from a single large earthquake provides a valuable opportunity to gain new insights into ground motion source, propagation and site effects. Studies of the characteristics of the Chi Chi ground motions conducted to date have examined the effects of closest distance to the fault, site condition, and the role of thrust of the hanging wall (e.g., Loh *et al.* [2], Chang *et al.* [3] and Wang *et al.* [4]). The objective of this paper is to evaluate and quantify the directivity effects in the ground motion records obtained from the 1999 Chi-Chi earthquake. The parameters evaluated are the horizontal-component peak ground acceleration (PGA) and the 5%-damped response spectral acceleration (PSA) at different periods.

Observations and inversions indicate that the Chi-Chi earthquake had a rupture length of about 100 km, a rupture width of about 48 km, strike of 3° , dip of 29° and rake of 66° (Ma *et al.* [5]). The pattern of surface deformation from the Chi-Chi earthquake varies along the Chelungpu fault, with progressively higher and wider fault scarps from the south to the north (Kelson *et al.* [6]). The southern portion of the fault showed relatively constant rupture velocity with an average slip of about 1 m, whereas the northern portion of the fault showed significant variations in velocity and produced a larger amount of slip, up to 8 m (Ma *et al.* [6]). Of 12 bridges that collapsed during Chi Chi earthquake, 9 of them were in the northern part of the fault rupture (Wallace *et al.* [7]). These facts suggest that the ground motions in the northern part of the fault were stronger than those in the southern part of the fault, and that rupture propagation effects towards the north were significant.

Directivity effects

It is widely recognized that ground motion amplitude is a function of earthquake magnitude and distance, site condition, faulting mechanism, hanging wall and footwall effects and possible directivity effects. The effects of earthquake magnitude, distance and site condition on ground motion amplitudes have been quantified in many empirical studies that have developed ground motion relations for various regions (e.g., see Abrahamson and Shedlock [8] and papers therein). However, it is only in recent years, with the collection of more extensive data sets, that it has become possible to empirically characterize the effects of faulting mechanism, hanging wall versus footwall, and directivity (e.g., Abrahamson and Somerville [9]; Somerville *et al.* [10,11,12]). In particular, it has been observed through recent earthquakes such as 1994 Northridge [11], 1995 Kobe [11] and 1999 Chi-Chi, Taiwan earthquakes that the ground motion amplitudes are enhanced in the direction of fault rupture propagation. Directivity effects are known to result in ground motions having higher amplitudes and shorter durations in the forward direction of rupture propagation (i.e., when the rupture propagates toward the site), while those in the backward rupture direction have reduced amplitudes and longer durations. Ground motions in the direction perpendicular to rupture propagation are not affected. There may also be significant differences between the strike-normal and strike-parallel components of horizontal ground motion amplitudes. For strike-slip faulting, the maximum of the radiation pattern for tangential S waves reinforces the directivity effects caused by rupture propagation toward the site, resulting in a large displacement pulse normal to the fault strike, as described by Somerville *et al.* [12]. For thrust earthquakes, the direction of the rupture propagation does not lead to reinforcement of the radiation pattern. Thus the strike-normal component is not necessarily larger than the strike-parallel component of horizontal ground motions. Preliminary analysis of the strike-normal to strike-parallel ratios for the Chi Chi earthquake did not show any significant effect, so this ratio was not evaluated further in this study; this is in agreement with a study by Wang *et al.* [4]. The dimensions and the strike and dip angles of the fault, the direction of the slip (slip rake angle), and the hypocenter all play critical roles in determining the characteristics and amplitudes of near-fault ground motions. The role of these effects has been explored by Aagaard *et al.* [13].

Characterization of directivity effects has been the subject of several studies. Research conducted by Somerville *et al.* [10,12] to modify empirical strong ground motion attenuation relations to include the amplitude and duration effects of rupture directivity characterized the directivity effects for strike-slip and

dip-slip faulting separately. Somerville *et al.* [12] used ground motion data from 21 earthquakes, mostly in California, with magnitudes of 6 or larger to quantify average directivity effects in terms of ground motion amplitudes and durations, relative to standard ground motion relations for California. For dip-slip events, they examined just the directivity effects up-dip from the hypocenter, choosing not to model any along-strike component of the propagation process for stations off the ends of the fault. The large dataset obtained from the Chi Chi earthquake provides an opportunity to explore directivity observations in more detail for a large thrust earthquake, including effects both near and far from the fault.

REGRESSION OF GROUND MOTION DATA FOR DIRECTIVITY EFFECTS

Median ground motion relation for Chi Chi earthquake

Ground motion relations predicting peak ground motions and response spectral ordinates as a function of magnitude and distance are a key input to seismic hazard analysis. In this investigation we are dealing with a single earthquake only, and therefore we can only derive an event-specific ground motion attenuation relation, rather than a general relation. However, this is a useful exercise because the nature of this dataset allows us to characterize features that cannot be readily explored in ground motion regressions for multi-event datasets. In particular, we can use regressions of the Chi-Chi earthquake data to generalize the effects of directivity on ground motion amplitudes. Such generalizations can then be used to predict how empirical regression equations for future earthquakes might be modified to better account for such effects.

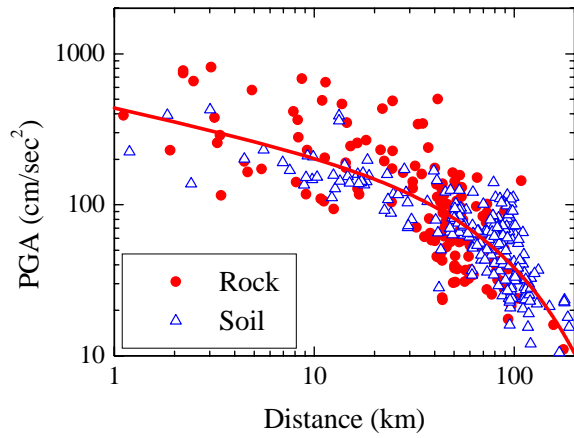
The ground motion parameters evaluated are the horizontal-component peak ground acceleration (PGA) and the 5%-damped response spectral acceleration (PSA) at six different periods (0.2, 0.5, 1, 1.5, 2 and 5 sec). We use average horizontal component in the regressions (where the average of the logs of the amplitudes is used). The ratio of the fault-normal to fault-parallel horizontal component was evaluated and found to be near unity, with the fault-normal component being on average just 10% larger than the fault-parallel component; thus we chose to regress just the average horizontal component. We start by determining the ground motion relations without considering the directivity effects. We use simple least squares to fit the observations to the form:

$$\ln Y = C_1 + C_2 \ln d + C_3 d + C_4 S \quad (1)$$

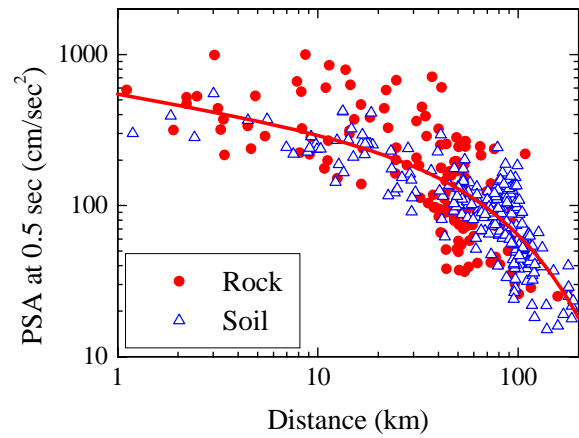
where Y is the ground motion amplitude in cm/sec^2 (PGA or $\text{PSA}(T)$), d is the closest distance to the fault rupture surface, and S is a site category factor ($S=1$ for soil sites, $S=0$ for rock sites). Natural log units (\ln) are used for the ground motion variables. C_1 , C_2 , C_3 and C_4 are the coefficients to be determined.

The 5% damped pseudo-acceleration response spectra were computed for 420 strong-motion records for natural periods up to 5.0 sec. The computations were made using the whole time-history record, after baseline correction. The response spectra were smoothed using a simple 9-point weighted triangular smoothing technique. The site condition factor is either 1 for soil sites or 0 for rock sites. The site classifications for stations with unknown site conditions were estimated from the spectral shape technique as described by Phung *et al.* [14,15]. Phung *et al.* [14,15] have also compared the classifications by this technique to classifications based on the interpretation of geologic maps and geomorphologic data as described by Lee *et al.* [16], and found general agreement. Among the 420 sites, 248 sites are classified as soil ($S=1$) and 172 sites are classified as rock ($S=0$).

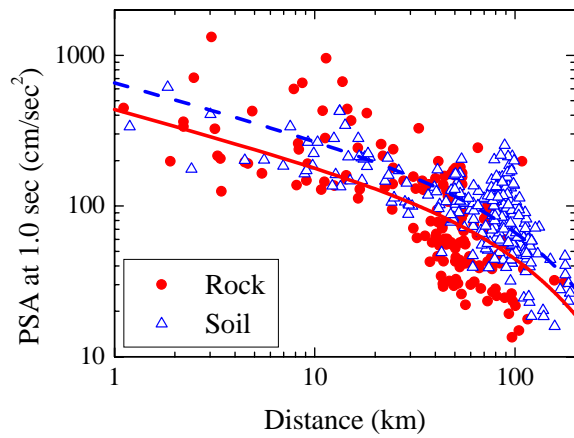
Observed ground motion amplitudes and the attenuation curves determined by the regression for PGA and PSA at 4 periods (0.2, 0.5, 1.0 and 2.0 sec) are plotted against the closest distance to the fault in Figure 1. The site condition factor coefficient C_4 for PGA and PSA at low periods is negligible (not statistically significant) and is therefore dropped from the regression. For higher periods the site effects become significant (factor of 1.8) for PSA.



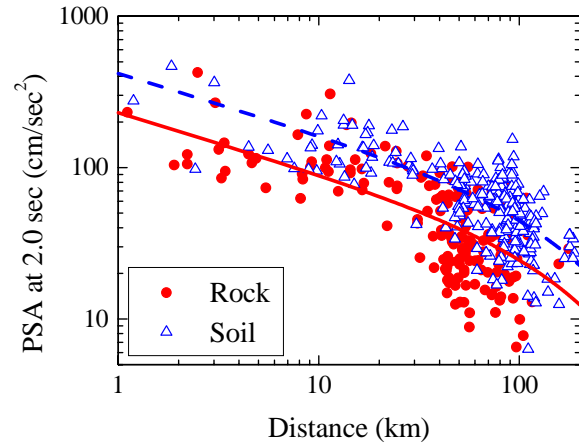
a) PGA.



b) PSA at 0.5 sec.



c) PSA at 1.0 sec.



d) PSA at 2.0 sec.

Figure 1. Observed ground motion amplitudes (symbols) and the regression curves for Equation (1) (Solid line for rock, dashed line for soil)

The coefficients of this regression to obtain median ground motion amplitudes for the horizontal component, without considering directivity effects, are given in Table 1.

Table 1. Coefficients of Equation (1) for the Chi Chi earthquake ground motions

Parameter	PGA	PSA at 0.2 sec	PSA at 0.5 sec	PSA at 1.0 sec	PSA at 1.5 sec	PSA at 2.0 sec	PSA at 5.0 sec
C_1	6.092	6.283	6.315	6.088	5.715	5.443	4.818
C_2	-0.293	-0.253	-0.231	-0.368	-0.387	-0.401	-0.417
C_3	-0.011	-0.012	-0.011	-0.006	-0.005	-0.004	-0.005
C_4	0.0	0.0	0.0	0.405	0.504	0.597	0.579

Analysis of results to obtain directivity effects

The residuals of the regression to Equation (1) are computed, where a residual is defined as the ratio of the observed ground motion value to the value predicted by Equation (1) (with coefficients given in Table

1). The map view of the computed ground motion amplitude residuals is plotted in Figure 2 for PGA. We observe large positive residuals along the fault on the east side (hanging wall side), and to the north of the fault, with negative residuals to the south. Plots for spectral parameters show the same trends. This shows a clear evidence of directivity effects on ground motion amplitudes.

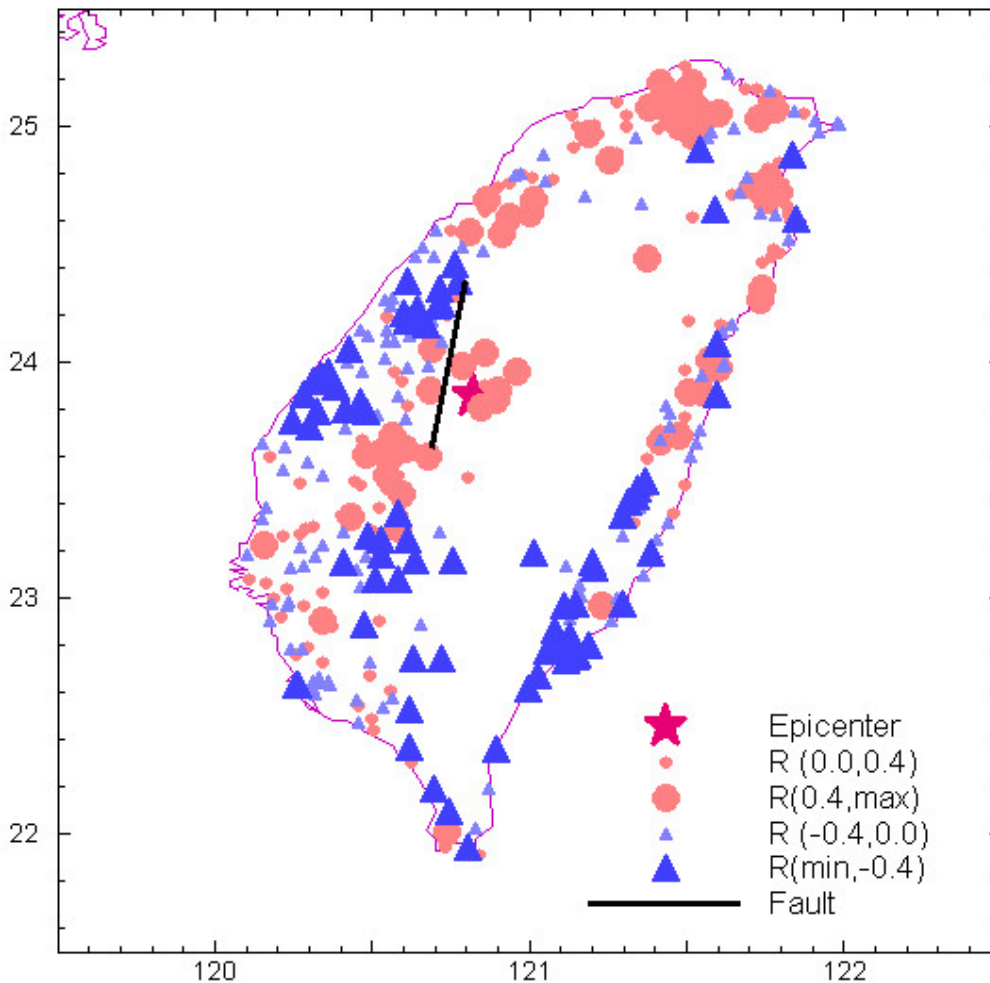
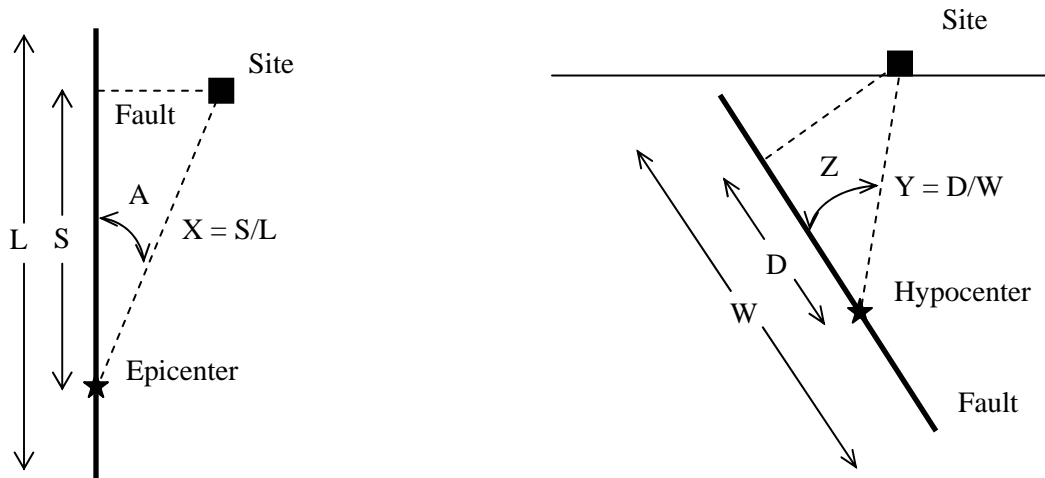


Figure 2. Map view of the residuals in \ln units (e.g., a residual of 0.4 represents an amplitude that is 50% larger than predicted).

The apparent directivity effects in the ground motion amplitudes are quantified by relating the computed residuals to directivity parameters. Following the conventions developed by Somerville *et al.* [12], it is expected that ground motion amplitude variations due to directivity effects will depend on two independent geometrical parameters: (i) the angle between the direction of wave propagation and the ray path of waves traveling from the fault to the site; and (ii) the fraction of the fault rupture surface that lies between the hypocenter and the site. The azimuth A and zenith Z angles and the fraction of the rupture fault surface that lies between the hypocenter and the site for along-strike and dip-slip components of rupture propagation are illustrated in Figure 3. It is noted that the directivity effects along-strike apply at all distances, while those up-dip apply only within the actual footprint of the fault rupture.



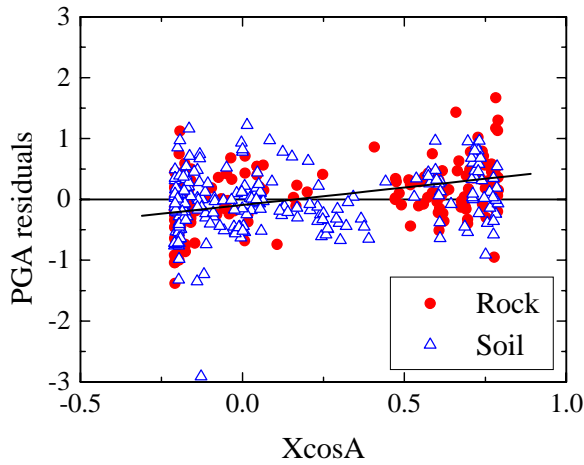
a) Along-strike (top view).

b) Up-dip (cross section).

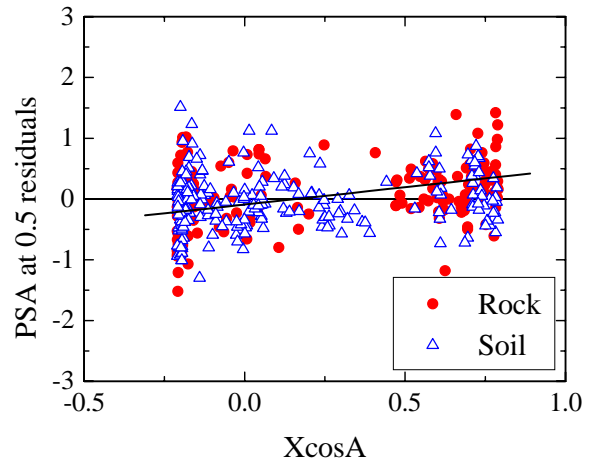
Figure 3. Definition of rupture directivity parameters A and X for along-strike (left) and Z and Y for up-dip (right) components of propagation (from Somerville *et al.*, 1997)

Somerville *et al.* [12] used near-fault ground motion data from 21 strong earthquakes to study the directivity effects on the ground motion amplitudes and duration using the function $X \cos A$ for strike-slip faults and $Y \cos Z$ for dip-slip faults. The cosine function was chosen because it provides a smooth decay of the ground motion values with increasing angle. In their study of directivity effects for dip-slip events, Somerville *et al.* [12] restricted their focus to sites near the fault, for which purely up-dip effects can be observed; they deliberately chose to exclude evaluation of the off-end effects of rupture propagation for dip-slip faults. In the present study, we use a variation of their approach to quantify the directivity effects of the Chi-Chi earthquake both near the fault (i.e., directly up-dip as in Figure 3b) and along strike (as in Figure 3a). To achieve that objective, we explore the effects of $X \cos A$ (as shown in Figure 4) and $Y \cos Z$ (as shown in Figure 5) on ground motion amplitudes separately. These effects should not be considered additive, because they have been examined separately (i.e., the residuals for the up-dip regression implicitly include any net along-strike effects). Thus they are alternative estimates of the magnitude of the potential directivity effects.

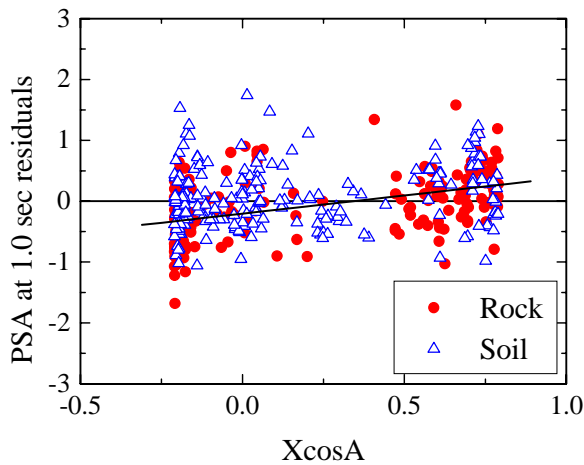
Figure 4 shows the variations of ground motion residuals of PGA and PSA at 4 periods (0.2, 0.5, 1.0 and 2.0 sec) with respect to $X \cos A$ for both rock and soil sites. In Figure 4, note the increasing trend of the residuals as $X \cos A$ increases. Both rock and soil sites to the south of the epicenter (i.e., $X \cos A < 0$) have more negative residuals, while sites to the north of the epicenter (i.e., $X \cos A > 0$) have more positive residuals. This agrees with the map view of the residuals as shown in Figure 2.



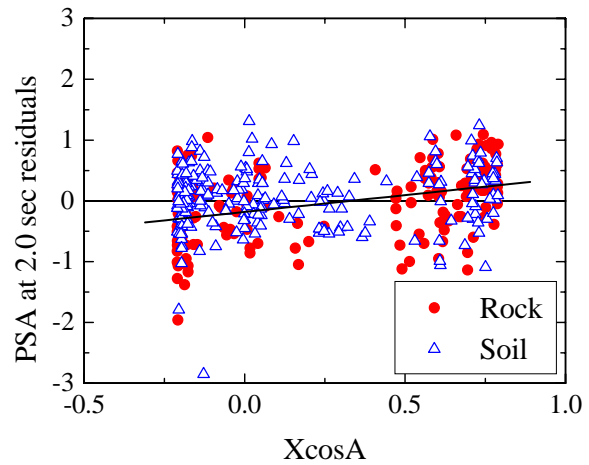
a) Residuals of PGA.



b) Residuals of PSA at 0.5 sec.



c) Residuals of PSA at 1.0 sec.



d) Residuals of PSA at 2.0 sec.

Figure 4. Variation of ground motion residuals with XcosA. Residuals are in ln units. Best-fit lines (Equation 2) are also shown.

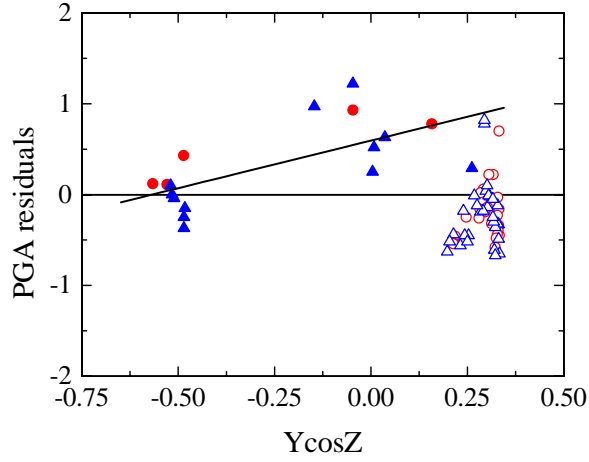
The residuals on Figure 4 were fit to:

$$R = B_1 + B_2 X \cos A \quad (2)$$

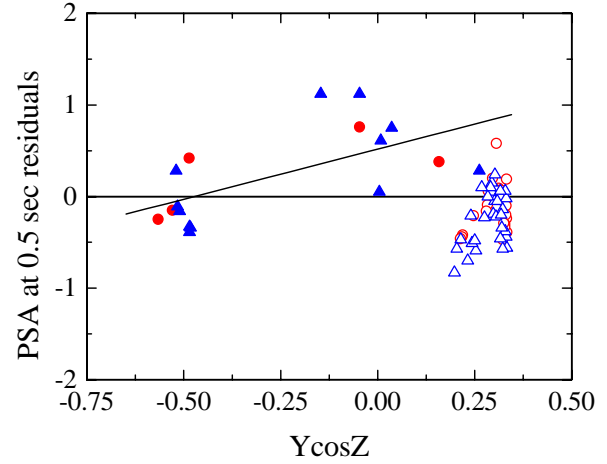
where R is the natural log of the residual; thus for PGA, $R = \ln \text{PGA}(\text{observed}) - \ln \text{PGA}(\text{predicted})$. X is the length ratio along strike and A is the azimuth (Figure 3). B_1 and B_2 are the coefficients, given in Table 2 along with their standard errors.

Table 2. Coefficients of directivity effects model along-strike ($R = B_1 + B_2 X \cos A$)

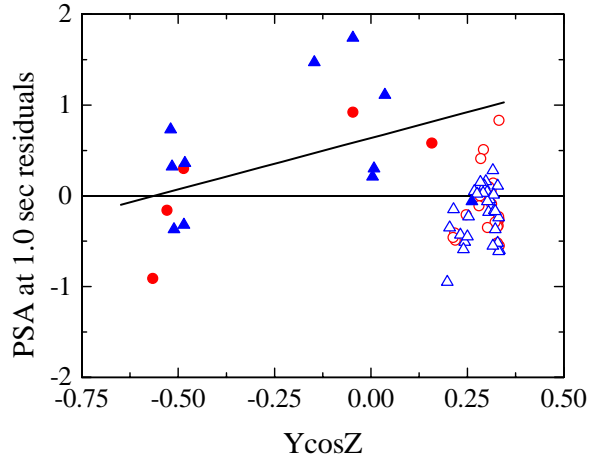
Parameter	PGA	PSA at 0.2 sec	PSA at 0.5 sec	PSA at 1.0 sec	PSA at 1.5 sec	PSA at 2.0 sec	PSA at 5.0 sec
B_1 and error	-0.082	-0.062	-0.067	-0.077	-0.070	-0.063	-0.075
	0.025	0.024	0.026	0.028	0.027	0.027	0.032
B_2 and error	0.464	0.346	0.381	0.433	0.397	0.354	0.426
	0.059	0.058	0.062	0.066	0.064	0.066	0.078



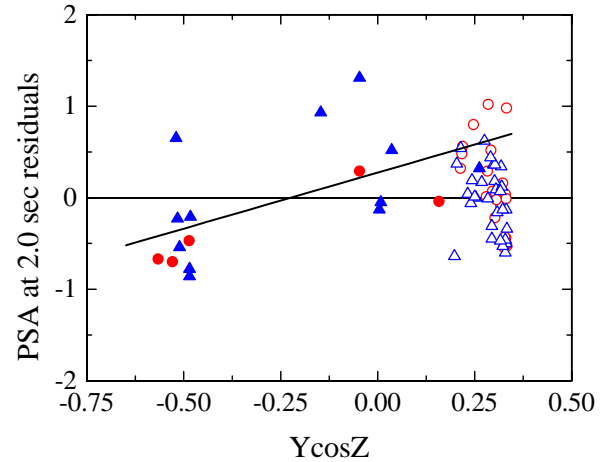
a) PGA.



b) PSA at 0.5 sec.



c) PSA at 1.0 sec.



d) PSA at 2.0 sec.

Figure 5. Variation of ground motion residuals with $Y\cos Z$. Residuals are in \ln units. Filled symbols are sites on the hanging wall; open symbols are sites on the footwall. Circles (red) are rock sites while triangles (blue) are soil sites. The best-fit lines for the hanging-wall residuals are also shown.

Figure 5 presents the residuals of PGA and PSA at 4 periods (0.2, 0.5, 1.0 and 2.0 sec), which examine up-dip directivity for stations within the overall fault footprint (within 50 km of the fault trace). Positive residuals are observed directly up-dip from the hypocenter (values of $Y\cos Z$ near 0) on the hanging wall. The data points on the left in Figure 5 (no apparent directivity effects) are from stations located further away from the epicenter (these are hanging-wall stations that would project onto the fault plane below the depth of the hypocenter). It is clear that there is a significant positive residual trend in $Y\cos Z$, but only for the hanging wall sites. The residuals of footwall sites cluster around zero, at a large value of $Y\cos Z$. In order to include the hanging wall effects for the dip-slip directivity, the residuals are fitted to:

$$R = HW (B_3 + B_4 Y\cos Z) \quad (3)$$

where Y is the width ratio and Z is the zenith angle (Figure 3). $HW = 1$ for sites on the hanging wall and $HW = 0$ for sites on the footwall. The coefficients B_3 and B_4 and their standard errors are listed in Table 3.

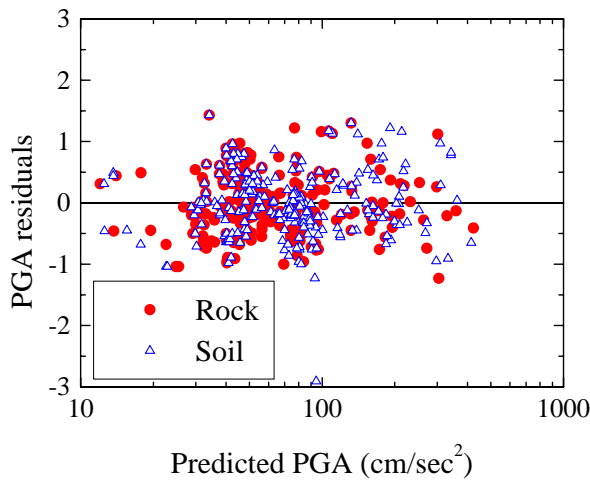
Table 3. Coefficients of dip-slip directivity effects model ($R=HW (B_3+B_4Y\cos Z)$). $HW=1$ for the sites on the hanging wall.

Parameter	PGA	PSA at 0.2 sec	PSA at 0.5 sec	PSA at 1.0 sec	PSA at 1.5 sec	PSA at 2.0 sec	PSA at 5.0 sec
B_3 and error	0.594	0.724	0.518	0.637	0.544	0.275	-0.132
	0.116	0.116	0.132	0.207	0.179	0.176	0.126
B_4 and error	1.048	1.301	1.094	1.134	1.248	1.224	1.109
	0.305	0.307	0.347	0.546	0.471	0.463	0.332

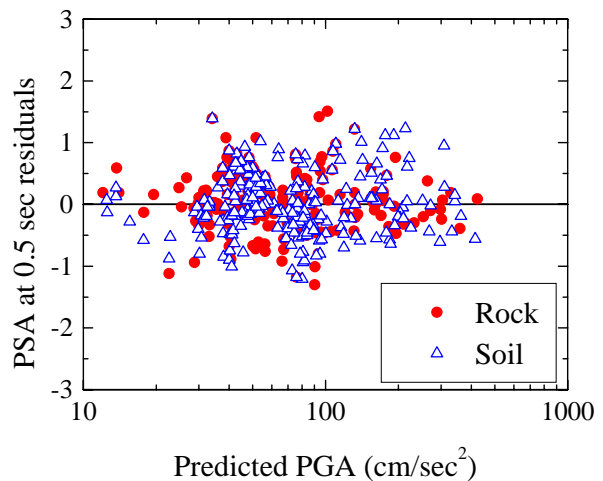
Results from Tables 2 and 3 suggest that directivity both along-strike and up-dip have a significant effect on the ground motion amplitudes. The ground motion amplitudes are approximately 1.5 times higher for sites in which rupture propagated strongly towards the site than those away from the site, along strike. Stations close to the fault up-dip from the hypocenter have strongly enhanced ground motion amplitudes, by a factor of about 2.7. These effects on amplitude are seen at all periods, and also for PGA.

Effects of ground motion intensity on the directivity models

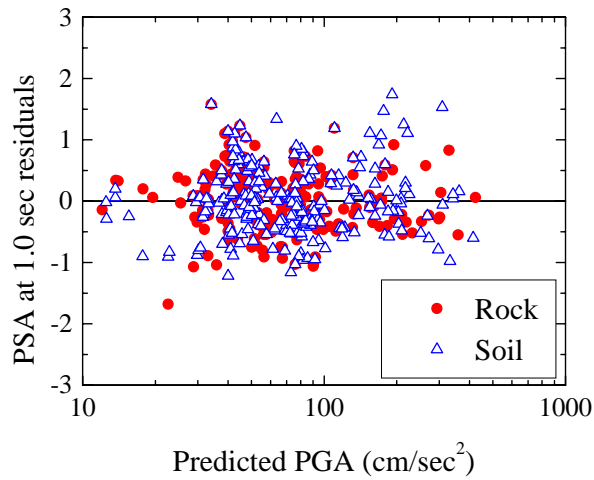
The directivity effects have been evaluated and quantified using 420 ground motion recordings from the Chi Chi earthquake. With the magnitude $M_w=7.6$, it is possible that nonlinear response has occurred at many soil sites during the Chi Chi earthquake. Nonlinearity is known to change the characteristics of ground motions. In this section we will explore the possible effects of ground motion intensity on the directivity models.



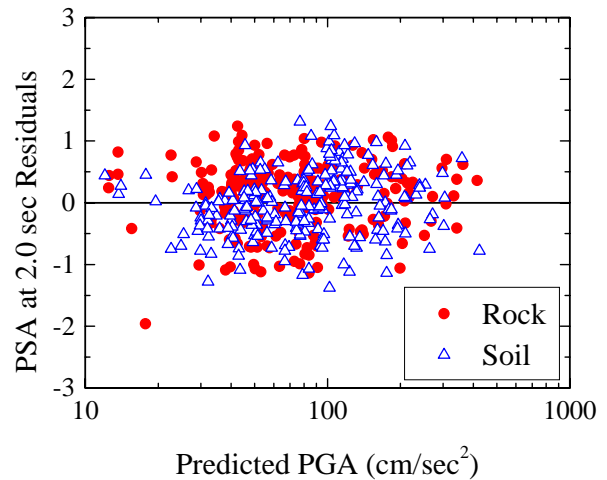
a) Residuals of PGA.



b) Residuals of PSA at 0.5 sec.



c) Residuals of PSA at 1.0 sec.



d) Residuals of PSA at 2.0 sec.

Figure 6. Effects of ground motion intensity (predicted PGA on rock) on residuals for rock sites (filled circles) and soil sites (open triangles). Residuals are given in ln units.

Figure 6 searches for nonlinear effects by plotting the ground motion residuals against the predicted PGA on rock (according to Equation 1) for each station. A decreasing trend of residuals with increasing PGA for the soil sites (relative to the residuals for the rock sites) would be expected if there was widespread nonlinear soil behavior. Such nonlinearity could potentially bias our results. From Figure 6, it appears that there are no residuals trends with increasing intensity level. We check this by regressing the residuals on soil to find a nonlinear factor, NL, given as:

$$NL = D_1 + D_2 \ln \text{PGA}(\text{Rx}) \quad (4)$$

where $\text{PGA}(\text{Rx})$ is the expected PGA on rock based on Equation (1), and D_1 and D_2 are the coefficients to be determined.

For PGA and all six spectral periods, we find that the coefficients D_1 and D_2 are not significantly different from zero. Thus there appears to be no significant nonlinear soil effects that could bias our results. The lack of soil nonlinearity may be due to the rather low PGA values for this earthquake. Typically, nonlinearity is observed for PGA values greater than about 100 to 200 cm/sec^2 (Beresnev and Wen [17]).

CONCLUSIONS

Directivity effects observed during the 1999 Chi-Chi, Taiwan earthquake were evaluated and quantified by using 420 ground motion records. The dip-slip component of the fault rupture propagation has a more significant influence on the ground motion characteristics than the along-strike component. This is expected as the Chi Chi earthquake was a thrust event. In the up-dip direction, ground motion amplitudes of the stations near the epicenter, towards which the rupture propagated, are enhanced by a factor of approximately 2.7. There is also a significant along-strike directivity effect. The amplitudes of PGA and PSA are approximately 1.5 times higher for sites in which rupture propagated strongly towards the site, along-strike. These results agree with those reported by Somerville *et al.* [12] in terms of the general magnitude of the directivity effects to be expected. However Somerville *et al.* [12] find that directivity effects grow steadily with increasing period, while for the Chi Chi earthquake we did not observe a trend with period. Furthermore we find that, even though the Chi Chi earthquake was a thrust event, there is a significant apparent directivity effect along strike. Large ground motions were observed to the north,

while weaker ground motions were observed to the south. More information on the soil conditions of the sites in these regions might shed further light on whether there are other possible explanations for these observations. However, it appears likely that the greater strength of the rupture propagation towards the north was a significant factor influencing the observed ground motions.

REFERENCES

1. Lee W. K., Shin T. C., Kuo K. W. and Chen K. C. (1999) "CWB free-field strong-motion data from the 921 Chi-Chi earthquake, Volume 1: Digital acceleration files on CD-ROM." Seismology Center, Central Weather Bureau, Taipei, Taiwan.
2. Chin-Hsiung Loh, Zheng-Kuan Lee, Tsu-Chiu Wu and Shu-Yuan Peng (2000) "Ground motion characteristics of the Chi-Chi earthquake Of 21 September 1999." *Earthquake Eng. Struct. Dyn.* **29**, 867-897.
3. Tsui-Yu Chang, Fabrice Cotton and Jacques Angelier (2001) "Seismic Attenuation and Peak Ground Acceleration in Taiwan." *Bull. Seism. Soc. Am.* Vol. **91**, No.5, pp. 1229-1246.
4. Wang, G. Q., Zhou, X. Y., Zhang, P. Z., and Igel, H. (2002) "Characteristic of amplitude and duration for near fault strong ground motion from the 1999 Chi-Chi, Taiwan Earthquake." *Soil Dynamics and Earthquake Engineering*, **22**, pp. 73-96.
5. Ma, K. F., J. Mori, S. J., Lee and S. Yu (2001) "Spatial and temporal distribution of slip for the 1999 Chi-Chi, Taiwan earthquake." *Bull. Seism. Soc. Am.* Vol. **91**, No.5, pp. 1069-1087.
6. Kelson, K. I., Kang, K. H., Page, W. D., Lee, C. T., and Cluff, L. S. (2001) "Representative Styles of Deformation along the Chelungpu Fault from the 1999 Chi-Chi (Taiwan) Earthquake: Geomorphic Characteristics and Responses of Man-Made Structures." *Bull. Seism. Soc. Am.* Vol. **91**, No.5, pp. 930-952.
7. Wallace J. (2001) "Chapter 8 Highway Bridges, Chi-Chi, Taiwan, Earthquake of September 21, 1999 Reconnaissance Report." *Earthquake Spectra*, Supplement A to Vol. **17**, 131-152.
8. Abrahamson, N. and K. Shedlock (1997). "Overview (of Special Ground Motion Issue)." *Seism. Res. L.*, **68**, 9-23.
9. Abrahamson N. A. and Somerville P. G. (1995). "Effects of the hanging wall and footwall on ground motion recorded during the Northridge Earthquake." *Bull. Seism. Soc. Am.*, Vol. **86**, No 1B, pp S93-S99.
10. Somerville, P., C. K. Saikia, D. Wald, and R. Graves (1995). "Implications of the Northridge earthquake for strong ground motions from thrust faults." *Bull. Seism. Soc. Am.*, Vol. **86**, pp. S115-S125.
11. Somerville, P. G. and Smith, N .F. (1996). "Forward rupture directivity in the Kobe and Northridge earthquakes, and implications for structural engineering." *Seismological Research Letters*, **67**(2), pp. 55.
12. Somerville, P. G., N. F. Smith, R. W. Graves, and N. A. Abrahamson (1997). "Modification of empirical strong ground motion attenuation relations to include the amplitude and duration effects of rupture directivity." *Seismological Research Letters*, **68**, pp. 180-203.
13. Aagaard, B., Hall, J. and Heaton, T. (2002). "Effects of fault dip and slip rake on near-source ground motions: Why Chi-Chi was a relatively mile M7.6 earthquake." PEER Report 2002/12. Pacific Earthquake Eng. Res. Center, Univ. of Calif., Berkeley.
14. Phung, V., Atkinson, G. M. and Lau, D. T. (2003) "Methodology for site classification estimation using strong ground motion data from 1999 Chi-Chi, Taiwan earthquake." (Submitted to *Earthquake Spectra*)

15. Phung, V., Atkinson, G. M. and Lau, D. T. (2004) "Methodology for site classification estimation using strong ground motion data from 1999 Chi-Chi, Taiwan earthquake." (Submitted to 13WCEE)
16. Lee C. T., Cheng C. H., Liao C. W., Tsai Y. B. (2001) "Site Classification of Taiwan Free-Field Strong-Motion Stations." *Bull. Seism. Soc. Am.* **91**, pp. 221-243.
17. Beresnev, I. and K. Wen (1996). "Nonlinear ground response - a reality?" (A review) *Bull. Seism. Soc. Am.*, **86**, 164-1978.